Journal of the European Ceramic Society 16 (1996) 745–752

0955-2219(95)00187-5
0955-2219/96/$15.00

Nickel–Alumina Bonds: Mechanical Properties Related to Interfacial Chemistry

P. Lourdin, D. Juvé & D. Tréheux

Ecole Centrale de Lyon, Laboratoire Matériaux, Mécanique Physique, URA CNRS 447 69131 Ecully Cédex, France

(Received 13 March 1995; revised version received 5 October 1995; accepted 12 October 1995)

Abstract

Mechanical properties of solid state bonded $Ni–Al_2O_3$ interfaces have been investigated as a function of several bonding parameters (temperature, pressure, time) and purity of the starting alumina.

It has been shown that they depend upon the plastic deformation of the metal, on the damages induced at the ceramic surface and on both the nature and amount of interfacial phase that appears during the bonding process.

According to the processing conditions used, the nickel aluminate spinel has not been found at the interface, but it has been shown that bonding arises from the magnesium aluminate spinel or sodium magnesium silicate and that nickel silicide is formed on the nickel side of the bond near by the interface.

Les propriétés mécaniques d'interfaces $Ni–Al_2O_3$ obtenues à l'état solide ont été étudiées en fonction des différents paramètres d'élaboration (température, pression, temps) et de la pureté de l'alumine de départ.

Il a été montré qu'elles sont fonction de la déformation plastique du métal, des défauts créés à la surface de la céramique ainsi que de la nature et de la quantité de phase interfaciale qui apparait au cours du processus de liaison.

Compte tenu des conditions expérimentales utilisées, la spinelle $NiAl_2O_4$ ne se forme pas à l'interface mais il a été montré que la liaison s'établit par l'intermédiaire soit de la spinelle $MgAl_2O_4$ soit d'un silicate mixte de sodium et de magnésium et qu'un siliciure de nickel se forme dans le nickel près de l'interface.

1 Introduction

Modern engineering components that often contain a metal bonded to a ceramic have been subject to extensive studies according to the variety and the complexity of the phenomena controlling the mechanical behavior of the interface.

When solid state bonding is used to obtain a metal–ceramic interface, the fracture resistance measured by conventional tests (shear, tensile tests) strongly depends upon the defects present along the interface such as pores and unjoined areas,[1] damage and cracks induced either by thermal stresses[2] or by friction between the two materials[3] especially in the ceramic close to the interface. Chemical interactions at the interface also play an important role. It has been shown that contaminants at the materials surfaces such as carbon, sulphur and chlorine atoms generally reduce the adhesion.[4] On the other hand, during bonding, chemical reactions often occur at the metal–ceramic interface influenced by the materials themselves, the welding temperature and the atmosphere.[5–7] The bond quality depends upon the reactions and on the properties of the reaction products. In addition, the diffusion of the metallic species in the ceramic body can reduce the toughness of the ceramic close to the interface which then affects the mechanical resistance of the bond.[8] Since bonds are often exposed in service to both temperatures and environments different from the one used for their formation, chemistry at the interface is likely to change, as well as the mechanical properties.[9] The nickel–alumina interface made by solid state bonding has been the subject of many studies.[3,5,10–16] From a physical point of view, it has been shown that strong bonds can be obtained when intimate contact between the two materials is effective depending upon the plastic deformation of the nickel, that varies with the applied pressure. Consequently the yield strength of the metal (function of the temperature and fabricating conditions) has to be taken into account as well as the friction coefficient at the interface and the thickness of the metal bonded.[3]

From a chemical point of view, the conditions leading to a reaction between solid nickel and alumina are now very well known: the aluminate formation ($NiAl_2O_4$) requires a threshold concentration of oxygen dissolved in the metal which is of the order of 1/5 the solubility limit.[5] From a mechanical point of view, contradictory results are published in the literature. Ni–Al_2O_3 bonds are reported to be either strong[11,14] or weak.[12,13] In both cases, the mechanical properties obtained were explained by the presence of nickel aluminate spinel at the interface. This paper reports results of the mechanical properties of solid state bonded Ni–Al_2O_3 interfaces investigated at room temperature with flexure and tensile tests. It focuses on the interfacial chemical dependence of interfacial fracture resistance.

2 Experimental Procedure

Two kinds of polycrystalline alumina have been investigated in this study: A99 'standard' (S) and 'high purity' (HP) from SCT (Société des Céramiques Techniques, Tarbes, France) and used as sintered, the average roughness value being about 0·3 μm R_a. The compositions of the starting alumina powders are given in Table 1. In both cases MgO has been introduced to inhibit the growth of alumina grains on sintering.

The nickel used has the following composition: Cu<0·01, Si=0·14, C=0·051, Mn=0·08, Fe=0·98, Co<0·01, Ni balance. Push-out tensile test samples (Fig. 1) were fabricated in order to measure the fracture strength of bonds and the four-point bending test (delamination specimen) (Fig. 2) was also performed to measure the interfacial fracture energy G_c.

The Al_2O_3–Ni–Al_2O_3 assembly was solid state bonded in a dynamic vacuum (5 10^{-3} torr) in the range 1050–1410°C for 1–48 h, with an applied pressure varying from 2 to 21 MPa. The dimetral ratio r/t (radius/thickness) of the metallic foil was varied in the range of 5–25. The heating rate to the bonding temperature was 150°C/h, the cooling rate to room temperature was 200°C/h. The applied pressure was maintained during all the thermal cycle. Following mechanical testing, SEM observations coupled with EDS analyses and grazing incidence X-ray scattering (GIXS) were carried out on both alumina and nickel sides of the bond after the nickel has been removed by peeling to detect the presence of interfacial phases.

3 Results

3.1 Pressure and temperature effects

From push-out specimens made with S alumina, the trends in bond strength with applied pressure and temperature are shown in Fig. 3.

The bond strength firstly increases with increasing values of applied pressure and temperature, then decreases at constant time and r/t ratio. Thermally actived microdeformation and diffusion act simultaneously to achieve the contact between metal and ceramic.[17] Plastic deformation of the metal is needed depending on the applied pressure, the yield strength of the metal (function of the temperature, work hardening), the friction

Table 1. Analysis of Al_2O_3 powders

	A99 standard (ppm) (S)		*High purity (ppm) (HP)*	
	Specification	*Typical value*	*Specification*	*Typical value*
Na_2O	<800	700	<60	40
K_2O	<5	<15	<30	<20
CaO	<220	<180	<30	20
SiO_2	<560	400	<100	50
Fe_2O_3	<360	300	<30	<10
Cr_2O_3	<50	10	<30	10
MgO	2000		2000	

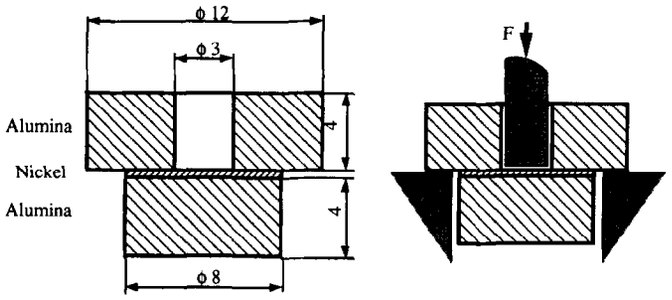

Fig. 1. Push-out specimen. Loading rate: 0·1 mm/min.

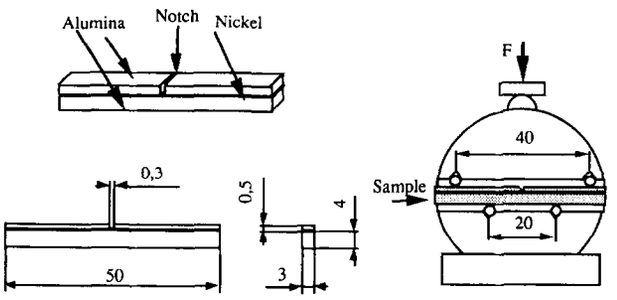

Fig. 2. Delamination specimen. Loading rate: 0·1 mm/min.

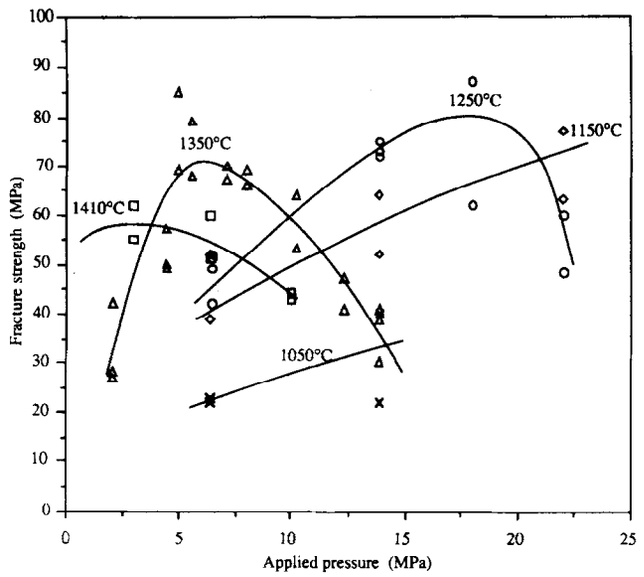

Fig. 3. Bonding strength versus applied pressure at different bonding temperatures, (S alumina).

coefficient at the interface and the dimetral ratio of the foil.[18] It can lead to full contact between the two materials without any overflowing of the metallic foil out of the interface. In these conditions, the maximum bond strength is obtained.

3.2 Influence of *r/t* ratio

It is shown in Fig. 4 that the parameter *r/t* acts on the bond strength in the manner described for both applied pressure and temperature. When the applied pressure is higher than that required to achieve the full contact, the metal is squeezed outside the interface. Sliding damages the outer junction ceramic surface by friction weakening the bond. Examples of such edge defects are shown in Fig. 5.

Whatever applied pressure, time and *r/t* ratio, up to 1150°C, bonds always fail within the interface. GIXS and EDS analyses performed on both

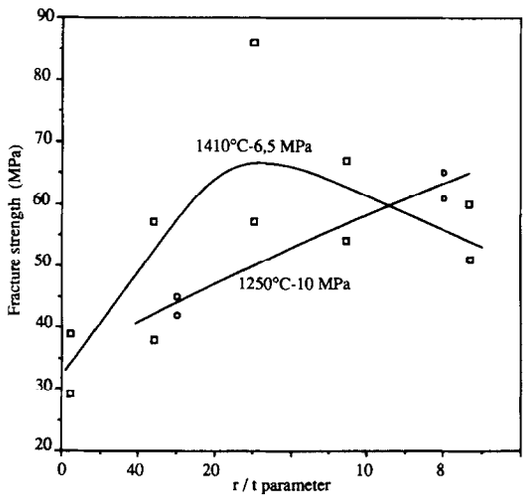

Fig. 4. Bonding strength versus *r/t* ratio (radius/thickness), (S alumina).

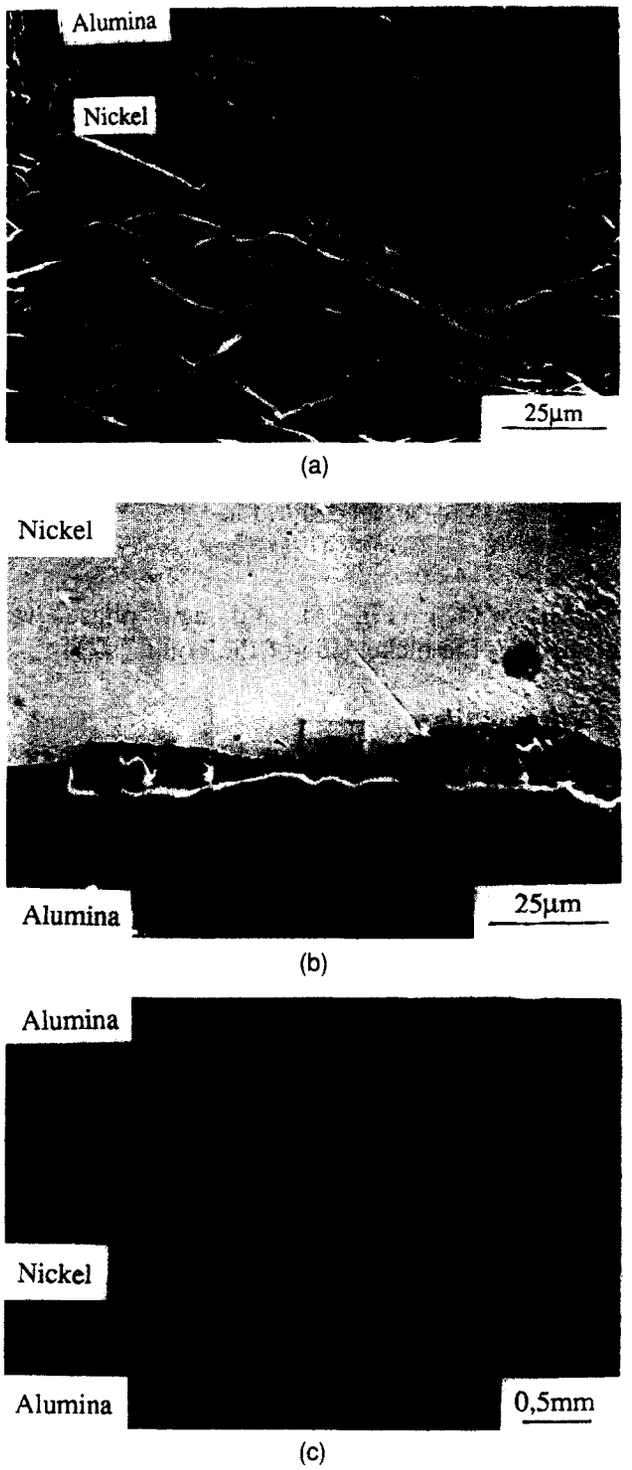

Fig. 5. Examples of flaws observed at the edge of Ni/S Al_2O_3 interfaces: (a) scratches on the nickel surface at high temperatures; (b) alumina grains detached by nickel on sliding at medium temperatures; (c) external 'chipping' of alumina at low temperatures.

alumina and nickel contact surfaces after a bonding time of 1 h indicate that only Al_2O_3 and Ni are present. Above 1150°C, the bonds fail within alumina at very different strength levels. At 1250°C and above, a crystalline film has been detected at the interface for a bonding time one hour long. Although the diffraction patterns were complex, the best fit between ASTM data and patterns was obtained for a sodium magnesium silicate

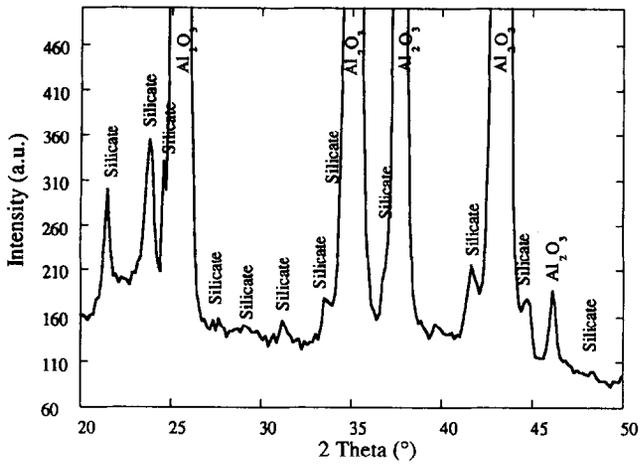

Fig. 6. GIXS diffraction pattern of standard alumina bonding area, (1350°C, 1 h).

($Na_2Mg_5Si_{12}O_{30}$) (Fig. 6). No new phase was detected on the nickel side of the bond.

3.3 Effect of time

Varying the bonding time at 1250°C, mechanical trends similar to those previously described were found (Fig. 7). In this case, the pressure chosen (6·5 MPa) was not suitable to produce a plastic macro-deformation of the metal. So the decrease observed in the bond strength associated to an interfacial fracture cannot be attributed to edge defects: other factors govern the mechanical resistance of the bond. SEM observations performed on the standard alumina side of bonds made after 10 and 48 h indicate that the contact area includes two zones having different morphologies, an inner zone (1), where alumina grains are badly defined and an outer one (2) where alumina grains are very well defined (Fig. 8). The extent of each zone varies with the duration of bonding, the inner zone being strongly reduced by the time. Some triple grain boundary points were found to be free of second phase, as previously observed by Drillet.[15]

GIXS analyses reveal after 10 and 48 h that the interfacial film corresponds to a spinel phase, $NiAl_2O_4$ or $MgAl_2O_4$, since both have the same lattice parameter. Nevertheless, as the characteristic blue colouration of $NiAl_2O_4$ was not observed, $MgAl_2O_4$ was assumed to be the compound present. It is confirmed by EDS analysis, since Mg has been detected in the bonding area but not Ni. Also, Mg concentration in the inner contact area was important while no Mg was detected in the outer area. Furthermore, no Ni, nor Ca, Si or Na were detected at the interface within the resolution limits of EDS (Fig. 9). On the nickel side of the bond a nickel silicide (Ni_3Si) was detected by GIXS.

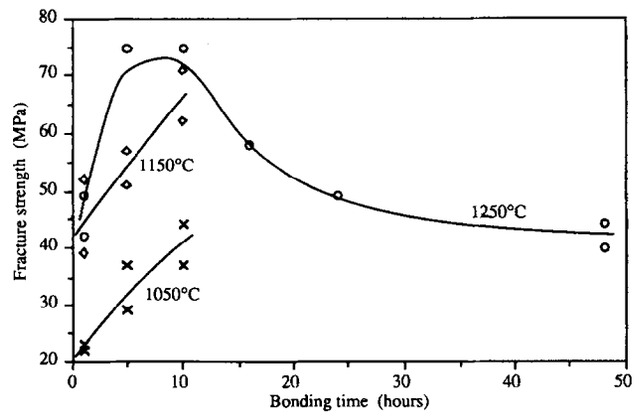

Fig. 7. Bonding strength versus bonding time. Applied pressure: 6·5 MPa, (S alumina).

In conclusion, for standard alumina, with a varying bonding time at 1250°C, it has been shown that the nature of the interfacial film changes from silicate, (1 h) to spinel, (5–48 h) and so the bonding strength which is first increased from 45 to about 75 MPa and then decreased to about 40 MPa, though the chemistry at the interface seems to be the same. According to the previous observations it is suggested that the interfacial area covered with $MgAl_2O_4$ (zone 1 Fig. 8) is responsible for the mechanical resistance of the bond. In support of this, the extent of zone 1 has been measured on bonds performed at 1250°C at 5, 10 and 48 h. Then the 'true' fracture strength was calculated with respect to the area measured but not to the macroscopic initial area (43·2 mm^2) of contact as for Fig. 3 (that leads to an apparent fracture strength). The results are given in Table 2. In all the cases the maximum strength value was obtained showing that the bond resistance is proportional to the area covered with $MgAl_2O_4$.

Using the four-point flexure delamination test[2] which has a mode mixity angle $\Psi \approx 45°$ (Fig. 2), the interfacial fracture energy of bonds made in the range 1050–1350°C was measured. It is shown in Fig. 10 that the maximum fracture energy (30 J m^{-2}) is reached at about 1150°C.[3] This temperature is the threshold temperature for the interfacial microstructure leading to the maximum bond strength to occur.

3.4 Role of alumina

Bonds made with high purity alumina with processing conditions identical to those precedently described, always fail within the interface at strength levels 30–60% smaller than those measured for standard alumina as shown in Fig. 11. As for S alumina, it is shown in Fig. 12 that the morphology of the HP alumina contact surface of a sample bonded at 1400°C during 1 h does not correspond to that of the starting polished surface and seems also covered with a phase. GIXS and EDS analyses indicate the presence of $MgAl_2O_4$ on the alumina side and of Ni_3Si on the nickel side of the bond (Fig. 13).

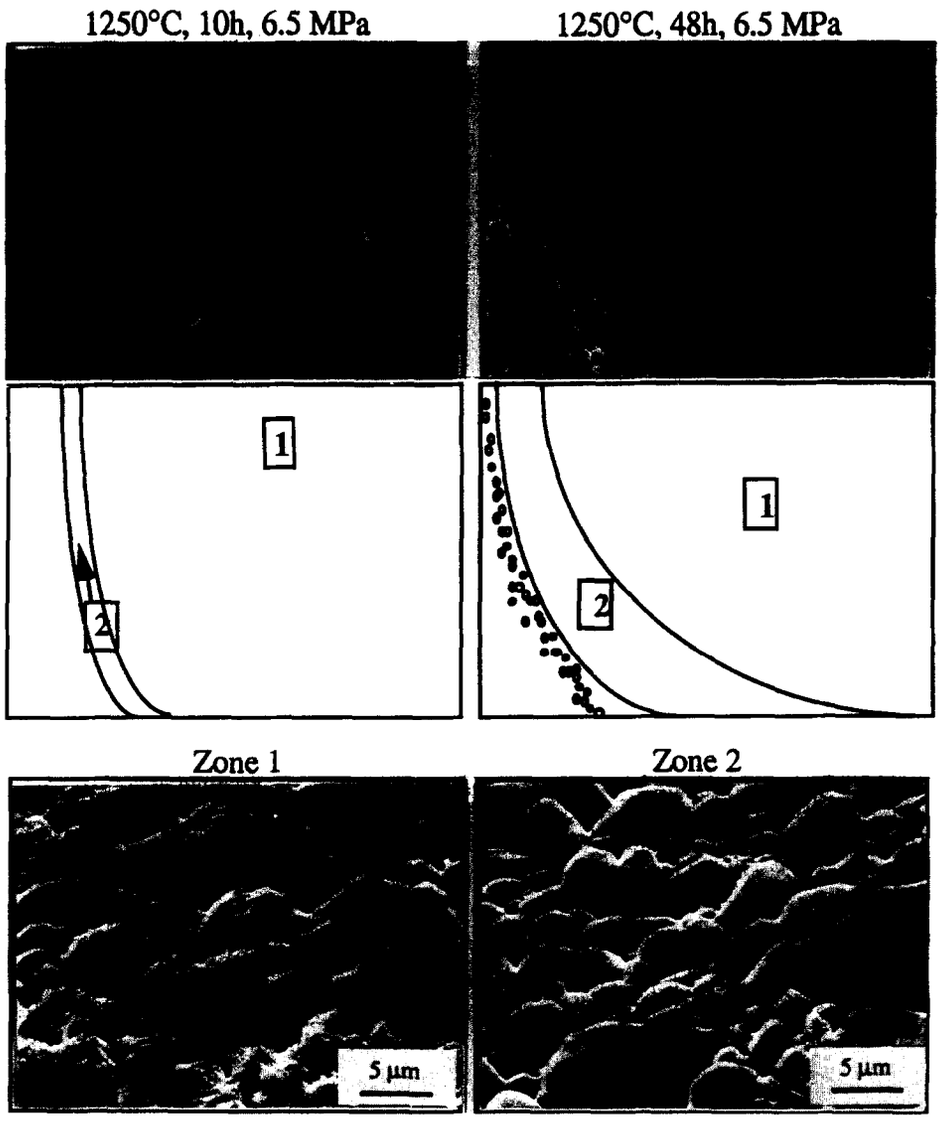

Fig. 8. SEM micrograph and repartition of zones 1 and 2 at the standard alumina interface.

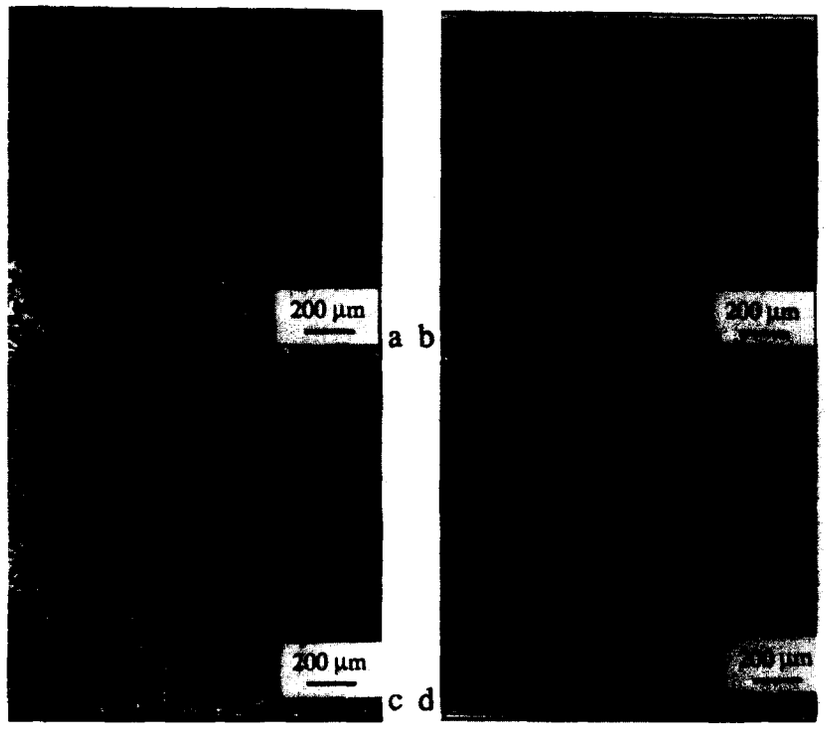

Fig. 9. Standard alumina area of contact after bonding at 1250°C under 6·5 MPa during 48 h: (a) SEM micrograph; (b) Mg map; (c) Al map; (d) Ni map.

Table 2. Fracture strength associated to the area covered with magnesium aluminate spinel

Time at temperature	*Surface of zone 1 (mm^2)*	*Fracture strength (MPa)*
	Maximum contact area:	
5 h 1250°C	43·2	75
10 h 1250°C	41·6	76
48 h 1250°C	35·5	60

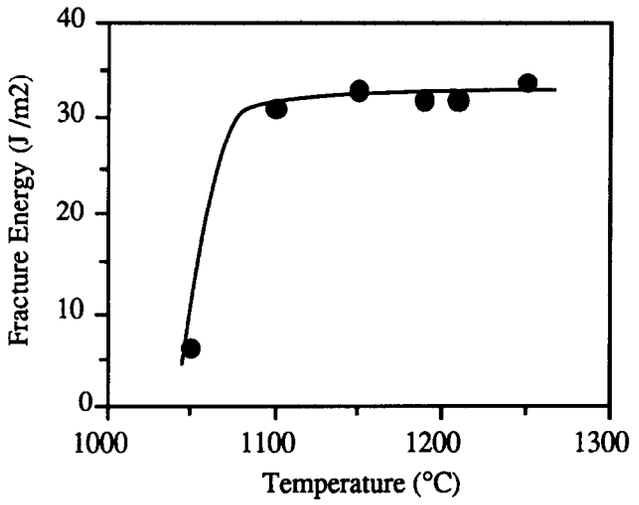

Fig. 10. Interfacial fracture energy versus bonding temperature. S alumina/Ni, 4 MPa, 0 h.

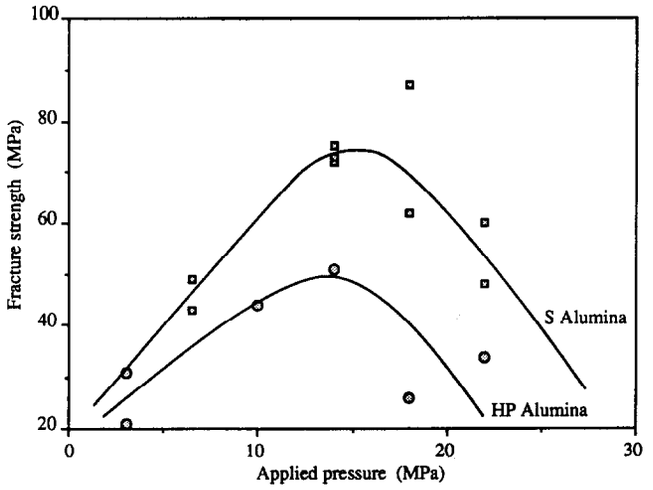

Fig. 11. Bonding strength versus applied pressure. 1250°C, 1 h, Ni = 0·5 mm (r/t = 5).

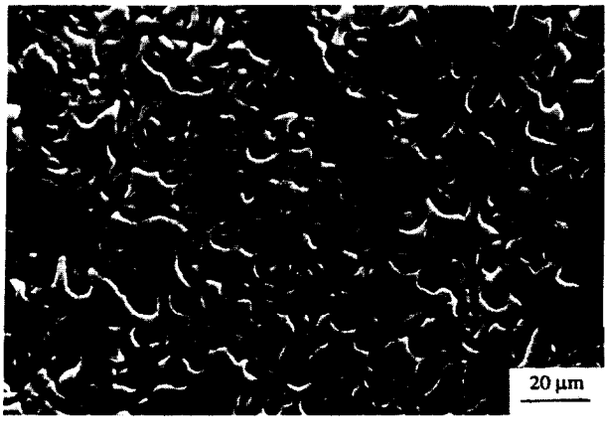

Fig. 12. SEM micrograph of high purity alumina bonding area.

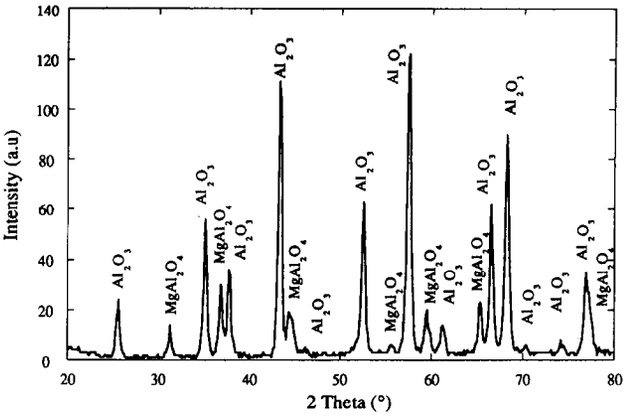

Fig. 13. GIXS diffraction pattern of high purity alumina bonding area (1400°C, 1 h).

4 Discussion

The experimental conditions used in this study to obtain Ni–Al_2O_3 bonds have not led to the formation of $NiAl_2O_4$ at the interface whatever the starting alumina (HP or S) but other, different phases have been identified.

Up to 1150°C, no new phases have grown at the interface on bonding, only nickel and alumina were observed.

Above 1150°C, it is suggested that a capillary mechanism acts firstly on bonding, favouring the migration of secondary phase material from the alumina triple grain boundaries points, allowing high concentrations of impurity at the interface. Then, reactions between the different components lead to the growth of new phases which vary with bonding time, temperature and alumina.

After 1 h, since 1250°C has been identified on the sides of the interface:

— in the case of HP bonds, magnesium spinel and nickel silicide
— in the case of S bonds, magnesium silicate and nickel

When bonding time is increased, magnesium spinel and nickel silicide have been observed for S bonds too.

The two aluminas studied contain the same amount of MgO, in return the quantity of SiO_2 is lower for the HP alumina than for the S alumina.

It is then propounded that the bonding arises firstly from magnesium silicate whatever the

purity of the starting alumina, the amount of which depends only on the initial SiO_2 level, the quantity of silicate formed being smaller with the HP alumina than with the S alumina. All the silicate has quickly transformed into spinel in the former, while it was always observed in the latter after a bonding time of 1 h.

Increasing bonding time diffusion mechanisms at the multiphase interfacial region and reactions between the alumina and the silicate lead to $MgAl_2O_4$, the silicon so released diffuses into nickel where it forms a silicide.

Towards the mode of fracture and the fracture strength measured, Ni–Al_2O_3 bonds also exhibit drastic changes with the solid state bonding variables and alumina purity. Such mechanical features can be connected with the nature and amount of the interfacial products formed, for bonds without edge defects.

SEM observations of S alumina contact area after a bonding time 1 h long, have shown that the alumina surface in the contact was progressively covered with magnesium silicate up to 1250°C. At this temperature the overall contact surface contains silicate and the maximum fracture energy G_c is reached (30J m^{-2}). Up to this temperature failures are adhesive (within the interface), above they are cohesive (within bulk alumina).

A major question is then asked: why does the $MgAl_2O_4$ become unstable in the time leading to debonding? The mechanism by which $MgAl_2O_4$ decomposes is not yet understood. It is suggested that oxygen is the determining factor since $MgAl_2O_4$ progressively disappears from the periphery to the middle of the junction: the outer region of the bond is in contact with an atmosphere having an oxygen level smaller than that required to stabilize the magnesium spinel. Such an hypothesis is consistent with other results and analyses that clearly show the critical role of oxygen in stabilizing spinels such as $CuAlO_2$, $NiAl_2O_4$ and $FeAl_2O_4$.[5–7]

5 Conclusion

The results presented raise the importance of both physical and chemical effects on the mechanical properties of metal–ceramic bonds examplified by Ni–Al_2O_3 interfaces.

From a physical point of view, to obtain strong Ni–Al_2O_3 interfaces using the solid state bonding process, a pressure leading to the greatest contact area between the two materials is needed. However it cannot give any flaws nor decohesion at the edge of the bond where high residual and applied stress are located. These defects acting as notches will be the fracture origin.[19,22]

From a chemical point of view, no direct reaction between Ni and Al_2O_3 has been observed. In our case (vacuum 5 10^{-3} torr), bonding depends only on the sintering alumina additives, especially MgO and SiO_2, capable of reaching the interface. Magnesium silicate and magnesium spinel have been observed at the alumina side and nickel silicide on the nickel side. It has been also shown that magnesium-based phases were metastable.

Mechanical properties of bonds are connected with the nature and amount of interfacial phases when physical defects are avoided. Providing that all the contact area between alumina and nickel is covered with an interfacial film magnesium silicate is associated with cohesive failures whereas magnesium spinel and nickel silicide lead to adhesive failures.

Acknowledgements

The authors wish to thank SCT for financial support and G. Thollet for EDS analyses.

References

1. Reimanis, I. E., Pore removal during diffusion bonding of Nb–Al_2O_3 interfaces. *Acta Metall. Mater.*, **40** (1992) S67.
2. Evans, A. G., Dalgleish, B. J., Charalambides, P. G. & Rühle, M., The fracture energy of bimaterials interfaces. *Mater. Sci. Engng*, **53** (1990) A126.
3. Lourdin, P., Les liaisons Ni/Al_2O_3 à l'état solide. Elaboration, état des contraintes thermiques, comportement mecanique. Thesis ECL No 92–31, 1992.
4. Korn, D., Elssner, G., Fischmeister, H. F. & Rühle, M., Influence of interface impurities on the fracture energy of UHV bonded niobium–sapphire bicrystals. *Acta Metall. Mater.*, **40** (1992) S355.
5. Trumble, K. P. & Rühle, M., The thermodynamics of spinel interphase formation at diffusion bonded Ni/Al_2O_3 interfaces. *Acta Metall. Mater.*, **39** (1992) 1915.
6. Trumble, K. P., Thermodynamic analysis of aluminate formation at Fe/Al_2O_3 and Cu/Al_2O_3 interfaces. *Acta Metall. Mater.*, **40** (1992) 105.
7. Béraud, C., Courbière, M., Esnouf, C., Juvé, D. & Tréheux, D., Study of copper-alumina bonding. J. Mater. Sci., **24** (1989) 4545.
8. Berroug, A., Juvé, D., Tréheux, D. & Moya, E. G., Silver–alumina solid state bonding: study of diffusion and toughness close to the interface. *J. European Ceram. Soc.*, **12** (1993) 385.
9. Allen, R. V. & Borbidge, W. E., Solid state metal ceramic bonding of platinium to alumina. *J. Mater. Sci.*, **18** (1983) 2835.
10. Klomp, J. T., Solid state bonding of metals to ceramics. *Science of Ceramics*, **5** (1970) 501.
11. Calow, C. A. Bayer, P. B. & Porter, I. T., The solid state bonding of nickel, chromium and nichrome sheets to α-Al_2O_3. *J. Mater. Sci.*, **6** (1971) 150.
12. Calow, C. A. & Porter, I. T., The solid state bonding of nickel to alumina. *J. Mater. Sci.*, **6** (1971) 156.
13. Vardiman, R. G., Preferred orientation of $NiAl_2O_4$ spinel grown on sapphire. *Mater. Res. Bull.*, **7** (1972) 699.
14. Bailey, F. P. & Bordidge, W. E., Solid state metal–ceramic bonding. *Mater. Sci. Res.*, **14** (1981) 525.

15. Drillet, P., Contribution à l'étude des liaisons céramique-métal: élaboration et étude structurale d'interfaces alumine/nickel. Thesis, University of Rennes, 1992.
16. Wan, C., Etude de la liaison métal-alumine élaborée par voies liquide et solide: mouillage, thermocompression. Thesis, University of Grenoble, 1992.
17. Derby, B., The formation of metal/ceramique interfaces by diffusion bonding. *Acta Scripta Metall. Proceedings series*, **4** (1991) 161.
18. Avitzur, B., Limit analysis of disc and strip forging. *Int. J. Mach. Tool. Des. Res.*, **9** (1969) 165.
19. Dalgliesh, B. J., Lu, M. C. & Evans, A. G., The strength of ceramic bonded with metals. *Acta Metall.*, **36** (1988) 2029.
20. Evans, A. G., Lu, M. C., Rühle, M. & Schmauder, S., Some aspects of the mechanical strength of ceramic/metal bonded systems. *Acta Metall.*, **34** (1986) 1643.
21. Mader, W. & Rühle, M., Electron microscopy studies of defects at diffusion bonded Nb/Al_2O_3 interfaces. *Acta Metall.*, **37** (1989) 853.
22. Dalgleish, B. J., Trumble, K. P. & Evans, A. G., The strength and fracture of alumina bonded with aluminium alloys. *Acta Metall.*, **37** (1989) 1923.